Water, Ice and Salts in the Solar System

Bryan Travis
Computational Geosciences Group
Earth and Environmental Sciences Division
Los Alamos National Laboratory
bjtravis@lanl.gov

Sea Ice Salinity Workshop
Santa Fe, New Mexico
September 8-10, 2010

Los Alamos

Saturn’s moon Enceladus

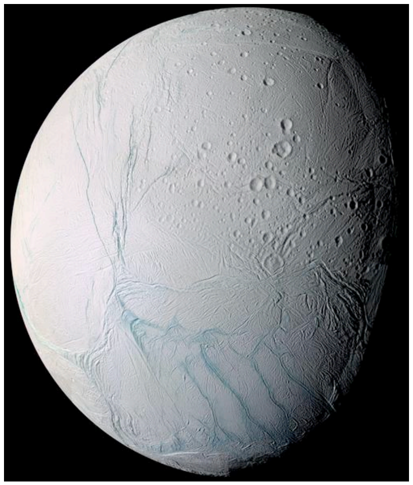

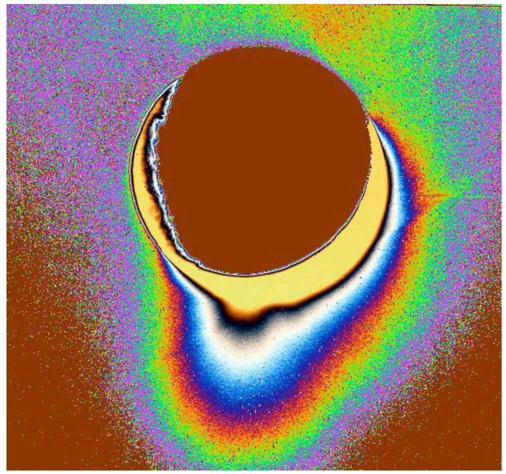

Enceladus is astonishing - very small (500 km diameter), yet very active: young, hot ‘tiger stripes’ (l); water geyser at south pole (r). (credits to Cassini team)

Enceladus must surely be differentiated, with a warm, permeable core and liquid ocean under an ice shell

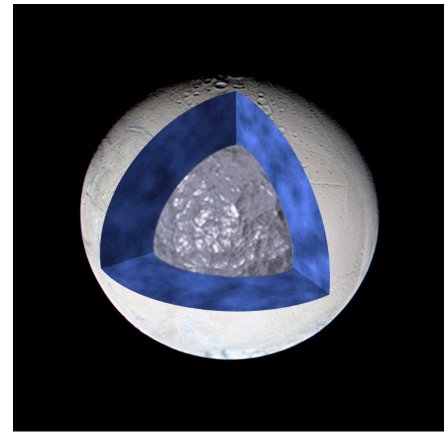

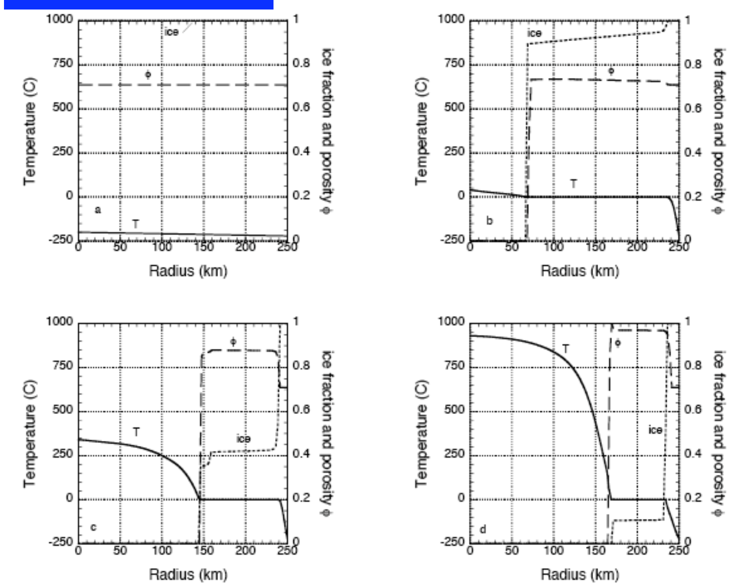

Simulation of evolution of dirty snowball to differentiated body - particles released by radiogenic melting of ice drift to center forming solid interior in a few Myrs -->

Los Alamos
NATIONAL LABORATORY
EST.1943

Europa - A Water Moon Revealing a Dynamic Ice Shell

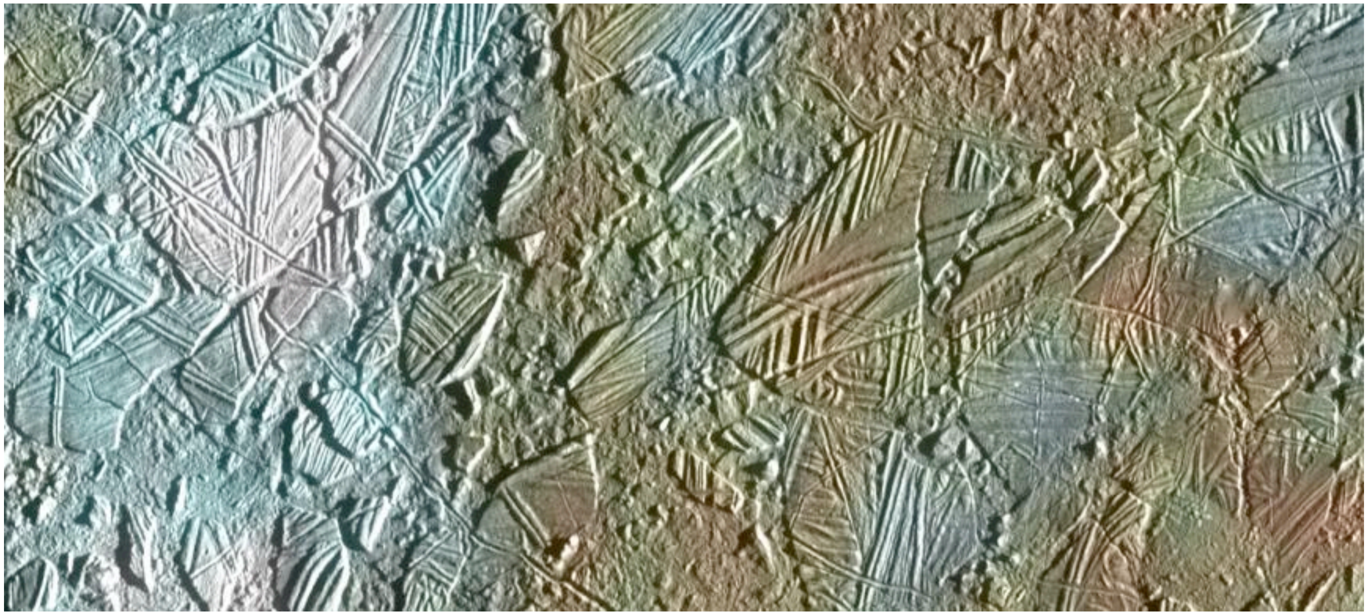

Left: North is to the top and the sun illuminates from the right. The image, centered at 9 °N, 274 °W, covers an area ~ 70 by 30 km.

Above: View of a small region of the thin, disrupted, ice crust in the Conamara region of Jupiter's moon Europa. The white and blue colors outline areas that have been blanketed by a fine dust of ice particles ejected at the time of formation of the large crater Pwyll some 1000 kilometers to the south. The unblanketed surface has a reddish brown color that has been painted by mineral contaminants carried and spread by water vapor released from below the crust when it was disrupted. This section of the surface appears to have experienced melting and refreezing in the not too distant past. Image courtesy of JPL.

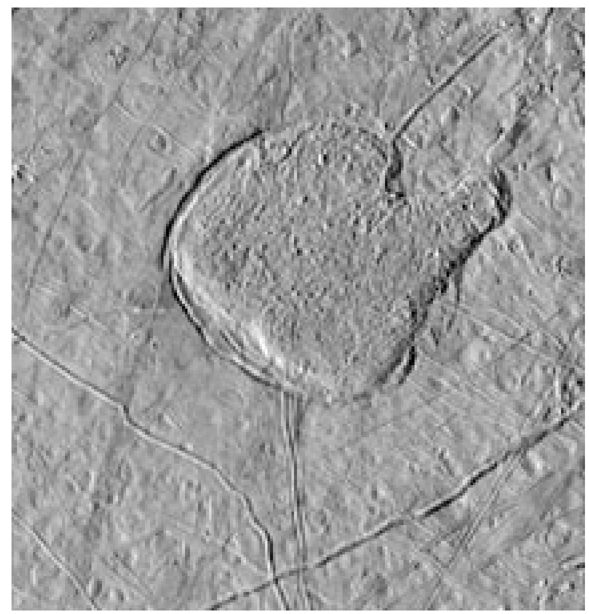

Right: Is this the surface expression of a convective plume? Central 'mitten' is about 100 km in diameter.

Current Model of Internal Structure and Transport Processes in Europa's Interior

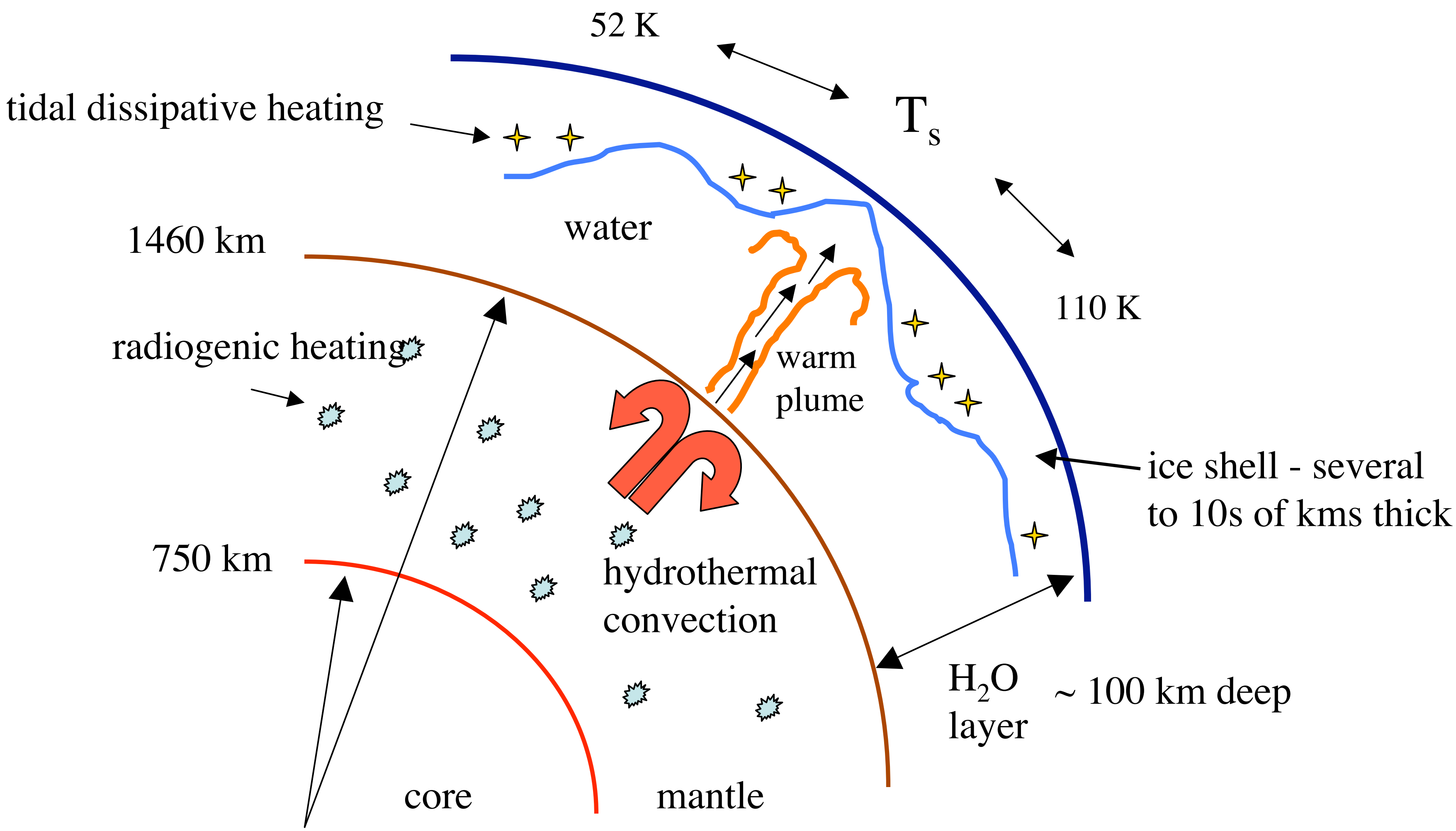

Los Alamos

Water activity spans Mars' entire history

- Noachian lakes, oceans
- Valley networks - surface flow erosion, groundwater sapping
- Polar caps and basal melting
- Fractures and outflows - e.g., Cerberus Fossae (20 Mya)
- Crater wall seeps, dark streaks (present era)
- Mineral deposits - hydrated salts
- Volcano environments - enhanced heat flow
- Rampart craters, equatorial rootless cones, soft crater walls
- Recently formed small craters with exposed ice lenses

Los Alamos
NATIONAL LABORATORY

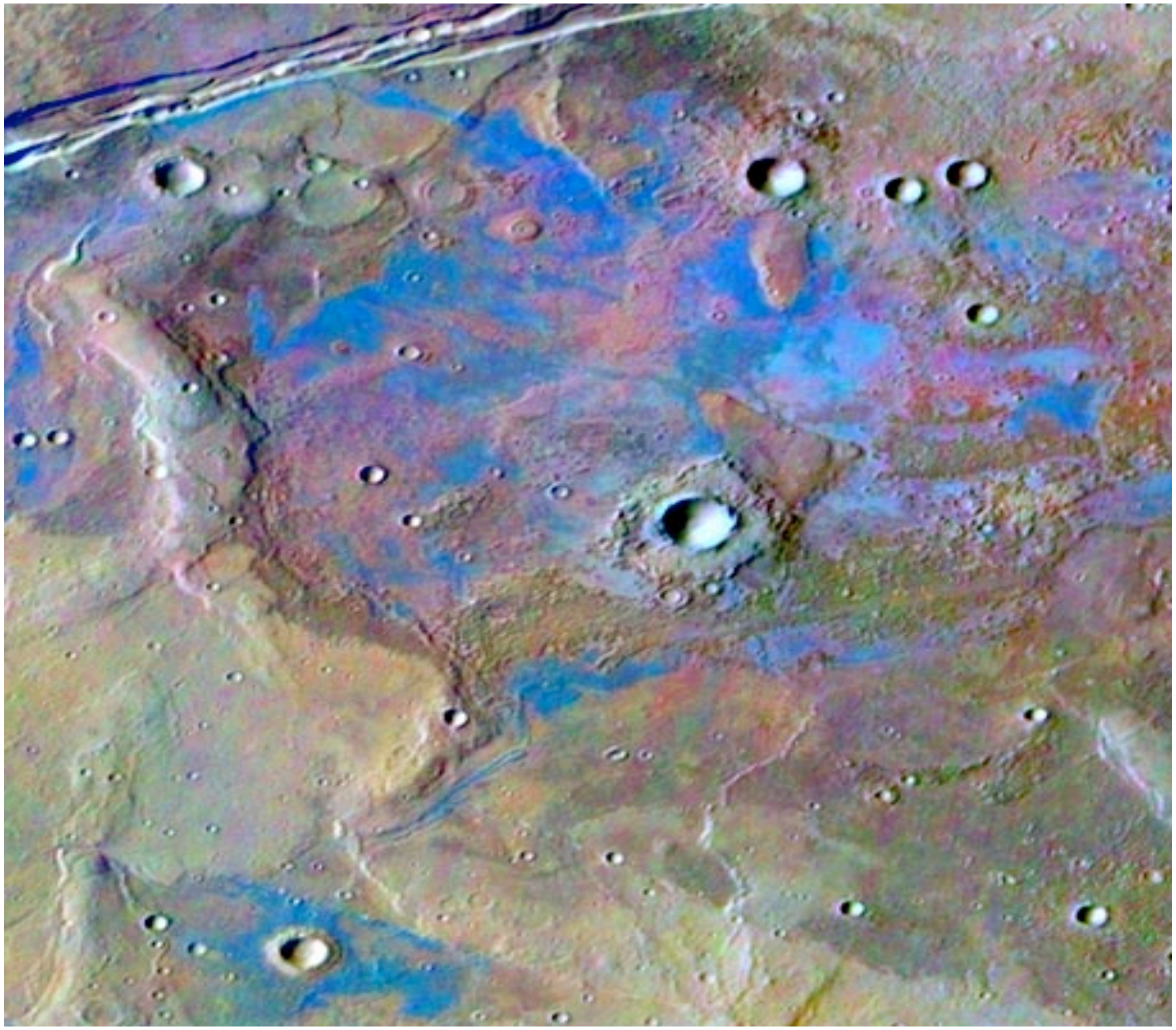

THEMIS DCS image (I08831002) of spectrally distinct region of southern highlands on Martian surface. As argued in Osterloo et al (Science 319, 1651, 2008), the blue color may correspond to chloride salt deposits.

Numerical Model of Flow and Transport in Porous Media with Phase Change

Darcy's Law $\mathbf{U} = - k/\mu\ (\nabla p + \rho_f\, g\, \mathbf{z})$ where $k = k_o(x,y,z)(1 - i)^3$

Mass Conservation $\nabla \cdot (\rho_f\, \mathbf{U}) = 0$

Energy Conservation

$$\partial/\partial t\ \{ (1-\phi)\, \rho_r\, c_r\, T + \phi(i\, \rho_{ice}\, c_{ice}\, T + \sigma\, \rho_{H2O}\, I_{H2O}) \} + \rho_{ice}\, Q_{ice}\, \partial i/\partial t + \nabla \cdot (\mathbf{U}\, E_w) = \nabla \cdot (K_T \nabla T)$$

where $\partial i/\partial t = \sigma \sqrt{(\beta/\pi)} \int_{T_1}^{T_2} \exp[-\beta(T - T_m(C))^2]\, dT$

Salt Conservation

$$\partial(\phi\rho C)/\partial\tau + \nabla \cdot (\mathbf{U}\rho C) = \nabla \cdot (D\rho\nabla X) + R(C)$$

Equation of State **H2O: Tables vs. T, P; linear in C**

Numerics: **Conservative Integrated Finite Differences; 1-D, 2-D or 3-D**

Constraint on Salt Concentration

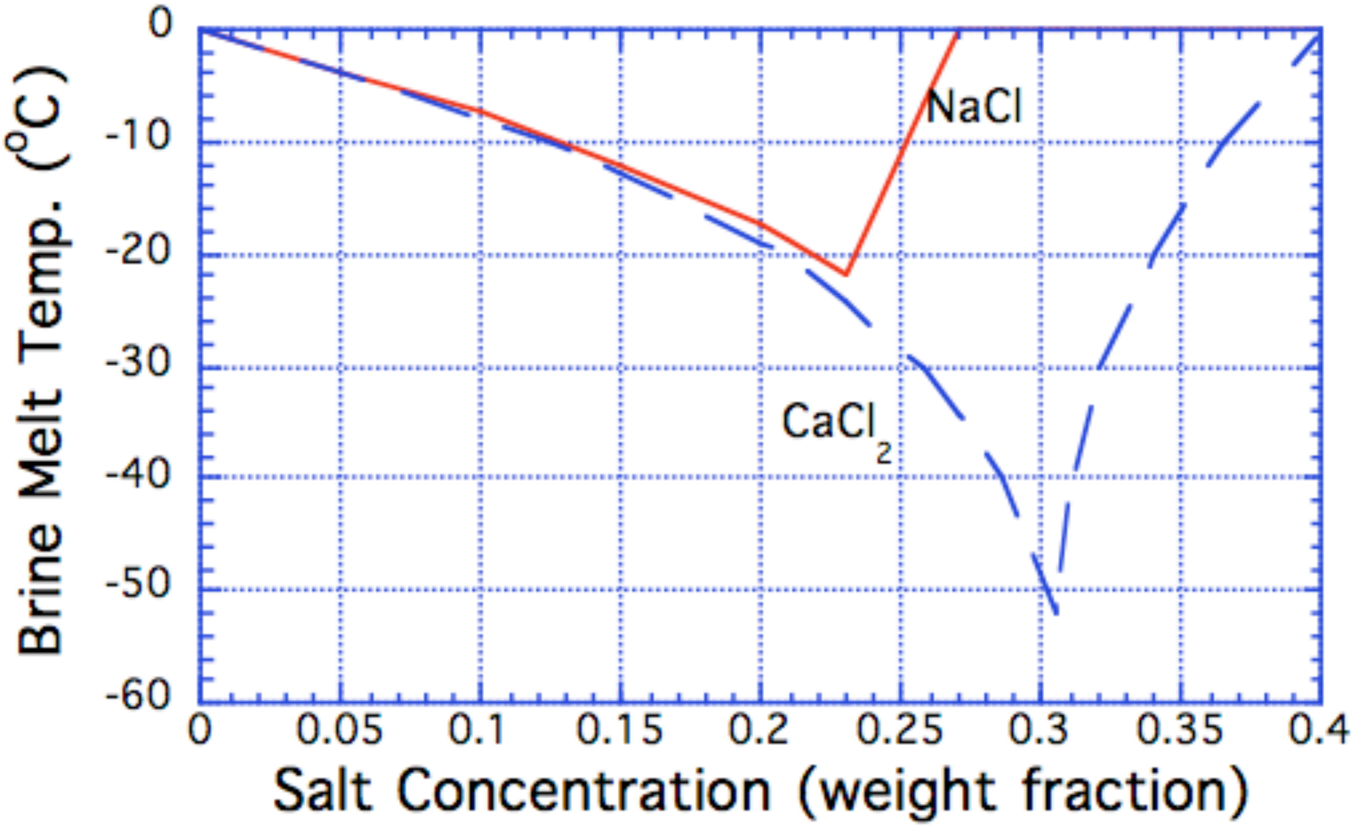

Additional constraints

$\sigma + i = 1, \quad \sigma\rho_w + i\rho_{ice} = \rho_{H2O}$

Solution procedure -

substitute Darcy's Law into mass continuity, solve resulting pde for pressure P;
compute velocity vector u; then transport heat and salt; then reconcile T and C;
repeat for next time step

approach to updating temperature T and salinity C:

for each computational cell -

salt mass M_c (new time) = M_c(prev time) + (advective flux + diffusive flux + reaction rate)* Δt

E(new time) = E (prev time)+ (advective flux + diffusive flux) * Δt

E(new time) = $(1-\varphi)\, \rho_r\, c_r\, T + \varphi\, \sigma\, I_w(T,P) + \varphi\, i\, c_{ice}\, \rho_{ice}\, T + \varphi\, Q_{ice}\, F(T-T_m(\, C\, (T, M_c\,)))$

apply Newton-Raphson iteration, with additional checks to keep solution in bounds and prevent endless cycling

usually converges in a few iterations; sometimes ten to twenty

Applications include:

Martian subsurface flow, infiltration and brines (Travis et al, JGR 2003; Feldman, LPSC 40)

Impact crater hydrological systems on Mars (Barnhart, Nimmo, Travis, Icarus 2010)

Experimental (McGraw & Travis, LPSC 37)

Asteroids, planetesimals coupled with chemistry and precipitation/dissolution (Travis, Schubert, Palguta - EPSL 2005; Palguta, Schubert, Travis, EPSL 2010)

Water moons Enceladus, Europa (Schubert, Palguta, Travis - Icarus 2007; LPSC 39)

Terrestrial - dike intrusions (Dutrow, Travis, Gable, GCA 2001)

Terrestrial - arctic permafrost, active layer gases

Images of Experiment

Thermocouple bank

Back side view

Insulated and running

<u>Box Dimensions</u>

Length = 1.5 m

Height = 0.5 m

Width = 0.1 m

Hydrothermal Convection

Rayleigh Number (Ra) for heat flux Q across bottom boundary

$$Ra = \rho \alpha g k D^2 Q / \kappa \mu \lambda$$

Ra uses min viscosity (μ) and max alpha (α) values for temperature range and depth-averaged permeability

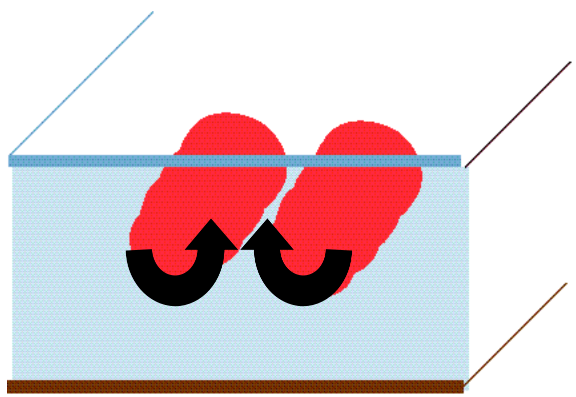

Low Ra - steady rolls

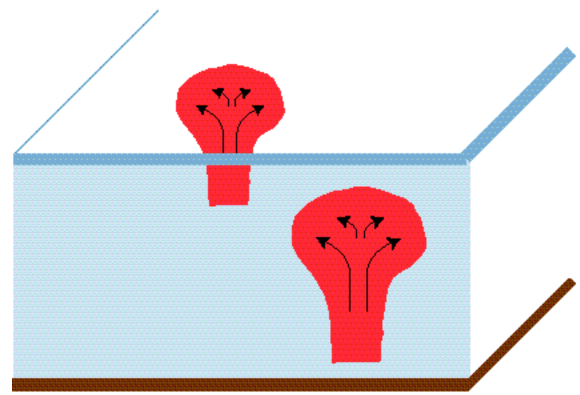

High Ra - unsteady plumes

Measured Viscosities of Salt Solutions vs Temperature and Concentration

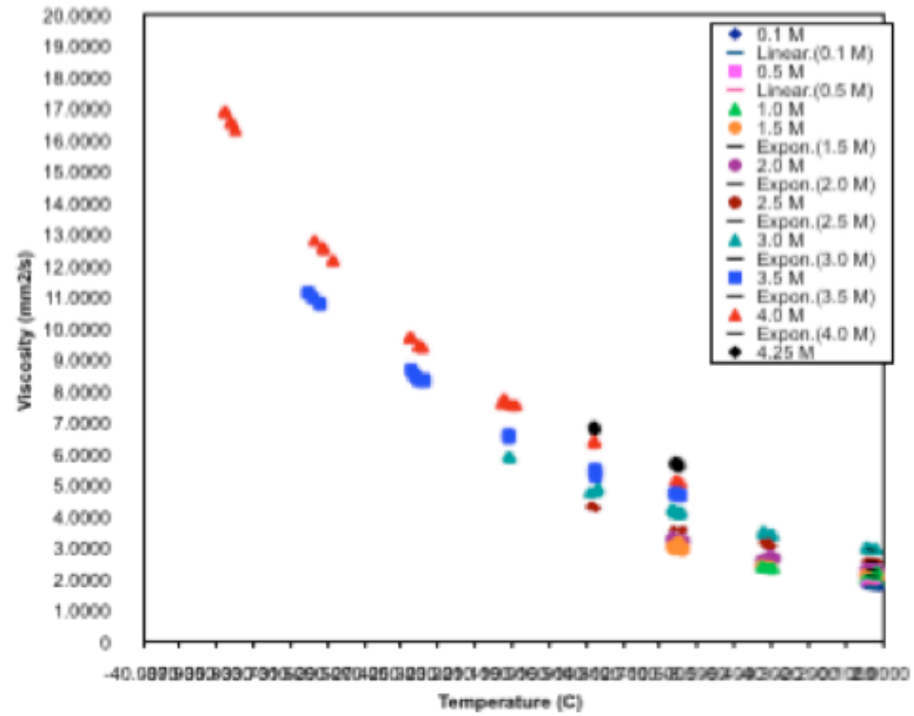

$CaCl_2$

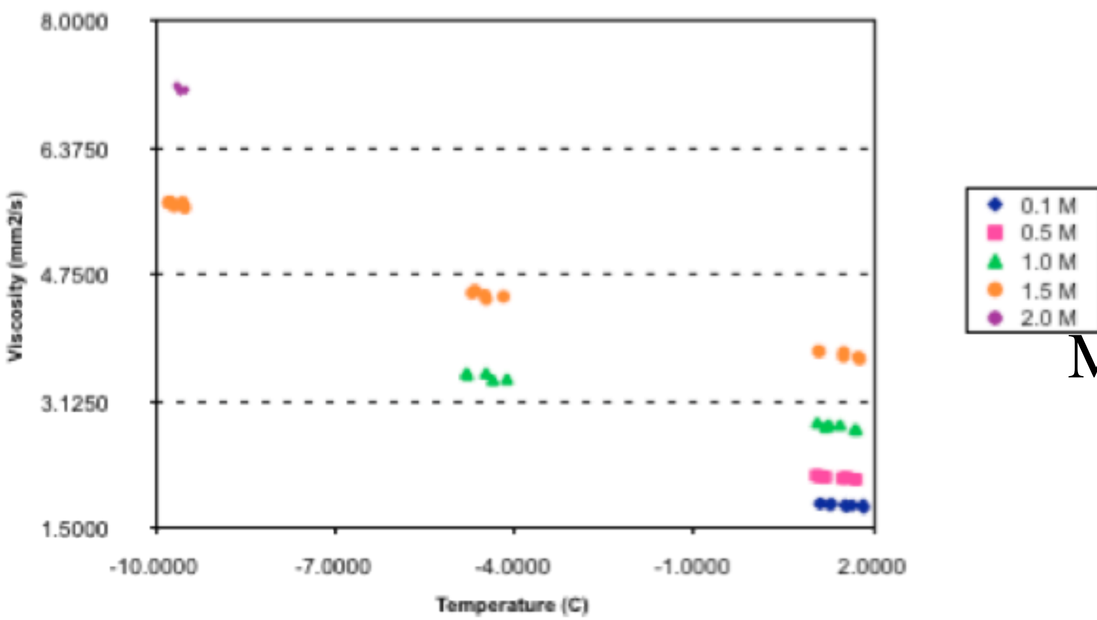

$MgSO_4$

M. McGraw & D. Reisenfeld
U. of Montana

$$Ra = \rho\beta kH\Delta Tg/\mu\alpha$$

ρ_l = density of liquid (g/cm^3)
k = permeability (cm^2)
ΔT = change in temperature (C)
μ = viscosity (g/cms)

β = thermal expansion of fluid (1/C)
H = height (cm)
g = gravity (cm/s^2)
α = thermal diffusivity (cm^2/s)

Experimental Parameters

$\rho = 0.99\ g/cm^3$
$\beta = 7.86 \times 10^{-5}/C$
$k = 4.9 \times 10^{-5}\ cm^2$
$H = 50\ cm$
$\Delta T = 25\ C$
$g = 979.115\ cm/s^2$
$\mu = 1.3 \times 10^{-3}\ g/cms$
$\alpha = 1 \times 10^{-2}\ cm^2/s$

$Ra = 3.6 \times 10^2$

Mars Parameters

$\rho = 0.99\ g/cm^3$
$\beta = 7.86 \times 10^{-5}/C$
$k = 1.2 \times 10^{-9}\ cm^2$
$H = 1 \times 10^6\ cm$
$\Delta T = 120\ C$
$g = 370\ cm/s^2$
$\mu = 1.3 \times 10^{-3}\ g/cms$
$\alpha = 1 \times 10^{-2}\ cm^2/s$

$Ra = 3.2 \times 10^2$

Below, temperature structure at starting point of experimental run. Upper right, temperature in experimental system, and lower right, simulated temperature, starting from temperature field in left image as initial condition. Base at 20 C.

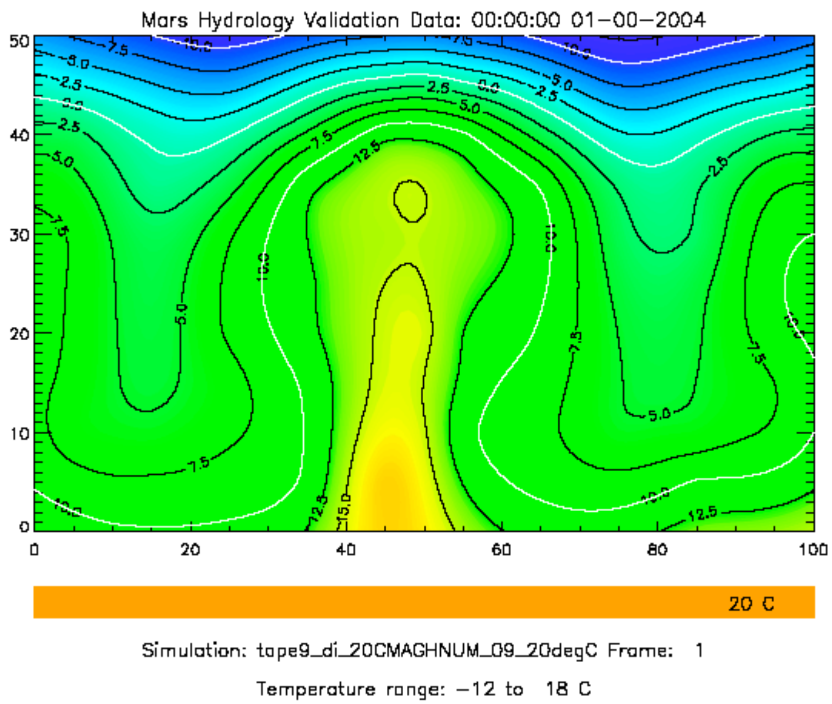

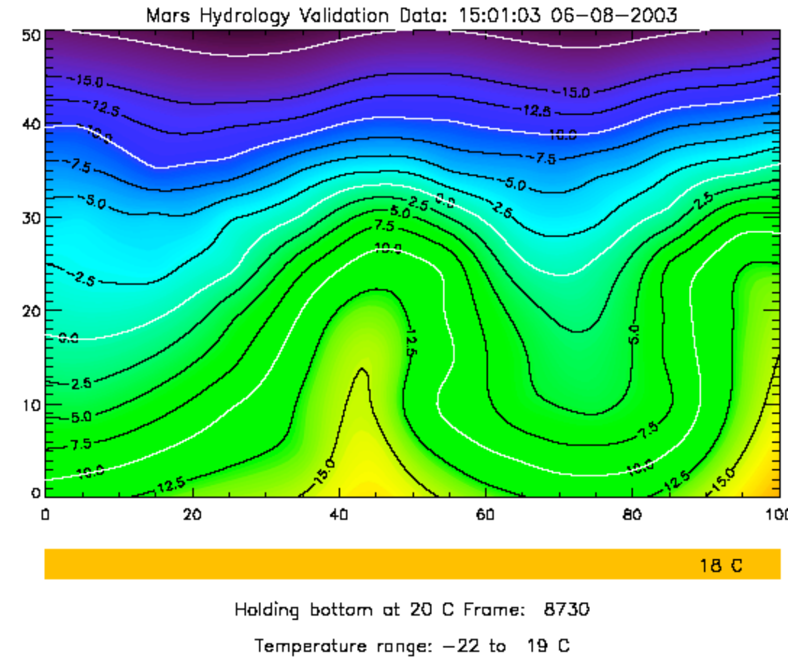

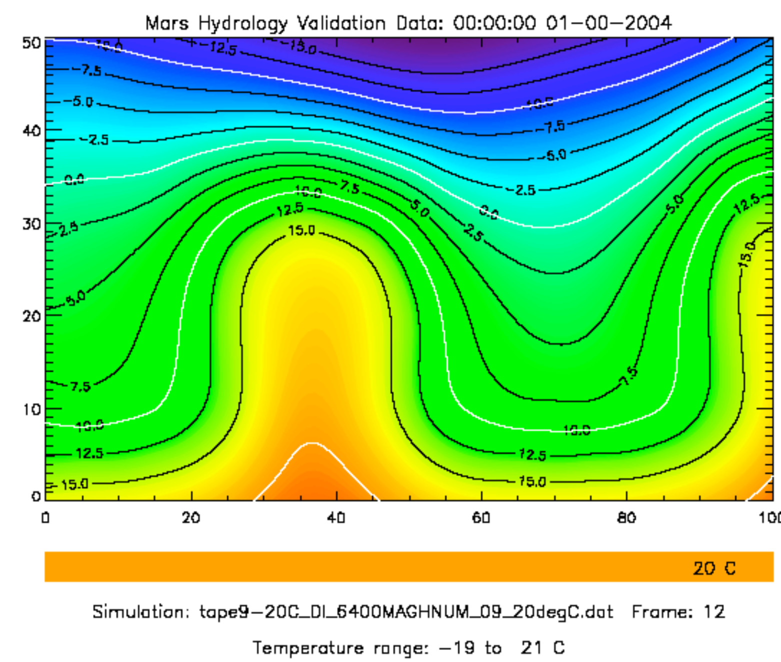

Starting point of experimental run is taken as that time after which the bottom temperature remains stable for several days. Right images are at start + 5 days.

Martian Subsurface Convection with Salt

Temperature Field

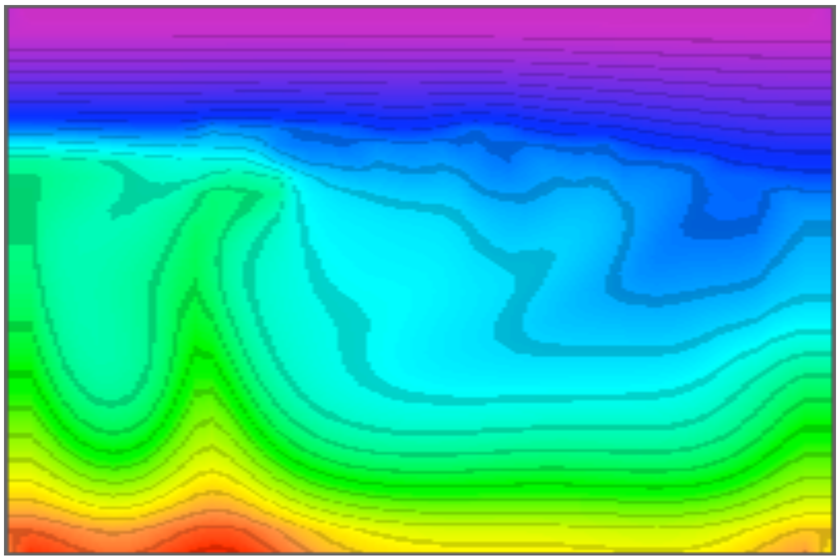

Water - Ice Field

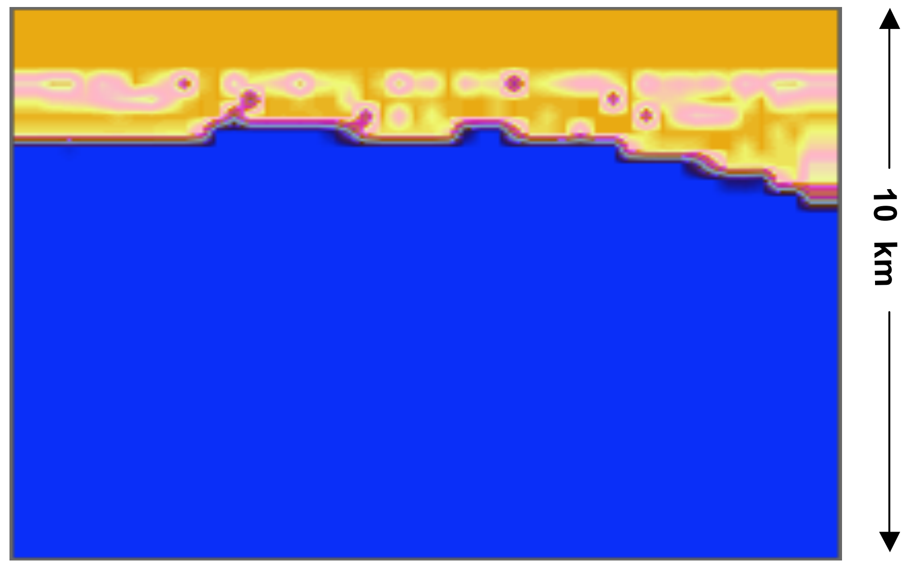

For Martian conditions (Ra # ~ 500) with 10% initial $CaCl_2$ concentration, MAGHNUM predicts an unsteady convective regime, a thinner cryosphere than for pure water, and a briny "mush" region between liquid water and completely frozen ice.

Hypothesized Near Surface Brine Systems on Mars

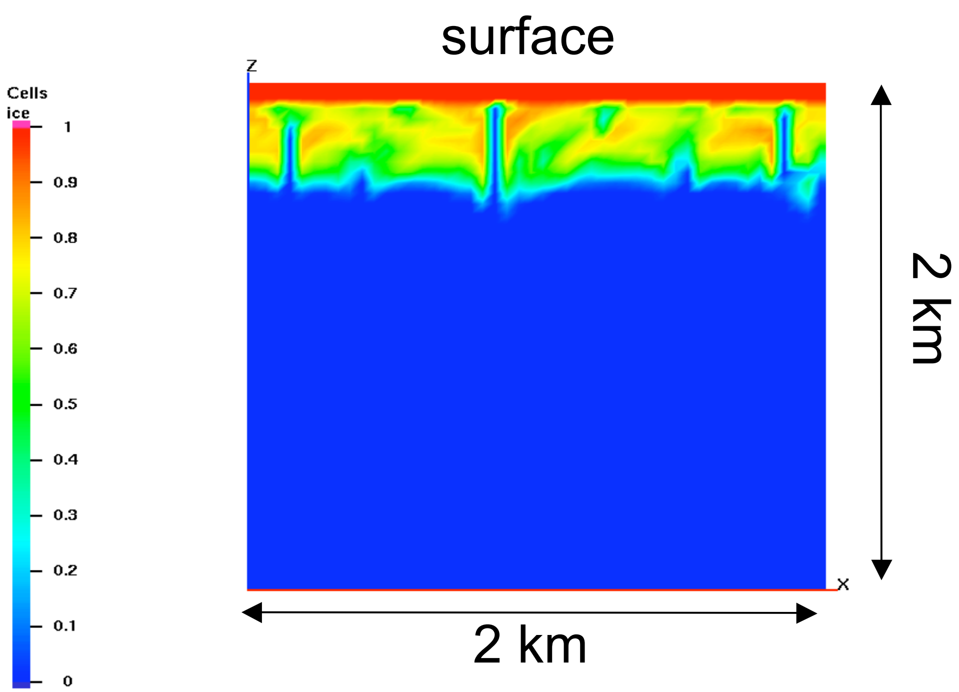

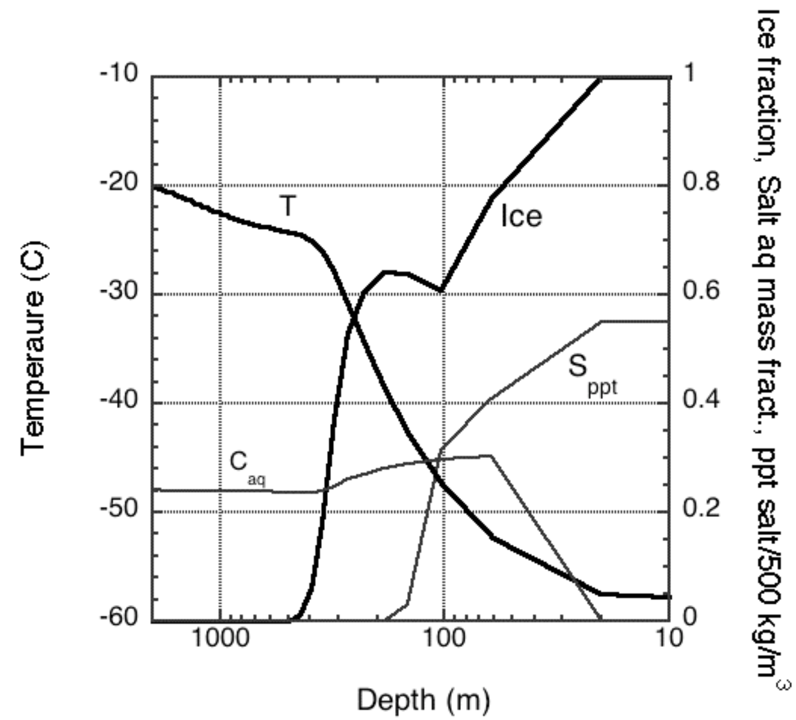

Left - Ice distribution after quasi-steady state has been established in a 2-D porous media simulation. Salt is $CaCl_2$, bottom heat flux of 40 mW/m^2. The dimensions of the system shown are 2 km across by 2 km deep. The upper 400 m are partially frozen. A roughly 75-100 m thick ice lens has developed at the surface. Narrow "drain pipes" form, with roughly 1 km spacing, that transport completely liquid brine back to the deeper aquifer. Right - Averaged profile of temperature (T), ice, aqueous (C) and precipitated (S) salt concentrations vs. depth. Hydrothermal convection driven by the geothermal gradient maintains an almost isothermal brine aquifer until the surface is approached. Without salt, the entire domain would be frozen.

Fraction of Pore Space Occupied by Ice

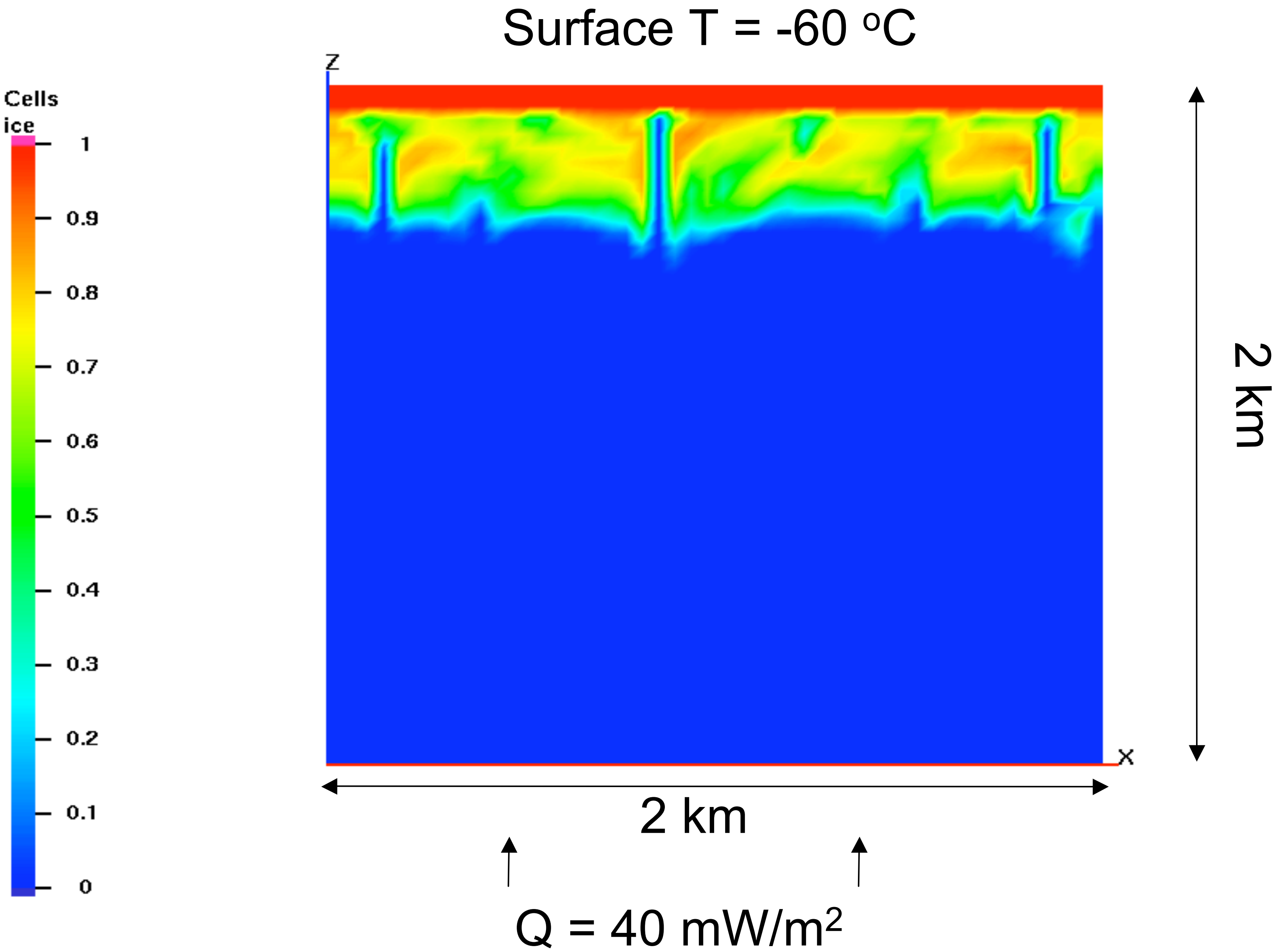

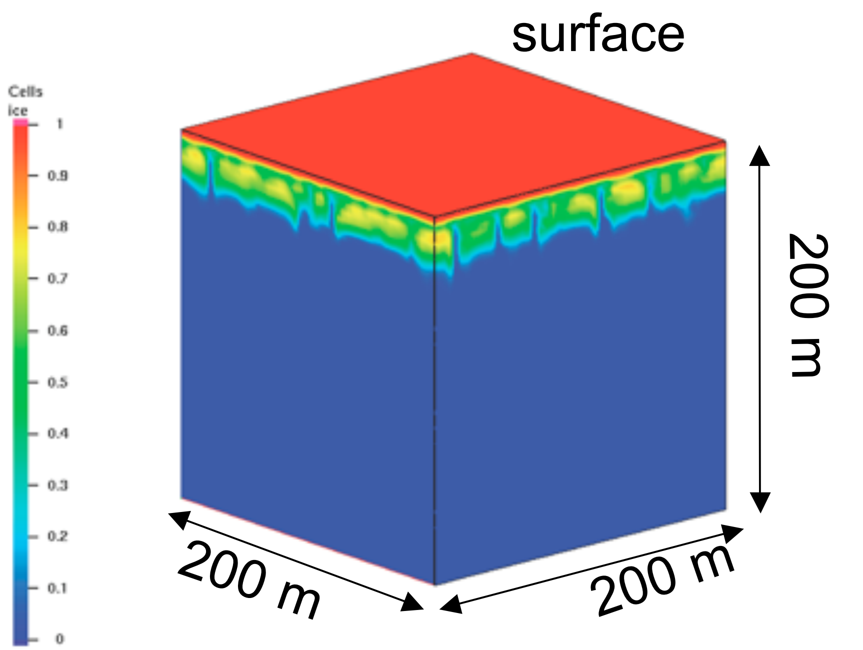

Brine Convection in Porous Medium - 3D

Snapshots of ice fraction - top left - the interior is almost completely liquid up to about 40 m below the surface, then a slush region occurs. Only the topmost 4 m is completely frozen. Top right, the upper 20 m have been removed. Bottom right, image is tilted to better show the polygonal arrangement of downwellings and drainage channels. Surface temperature is -55 oC; salt is $CaCl_2$. Quasi-steady pattern sets up in about 1,000 - 3,000 years after start-up from conductive temperature profile. Images shown are at 3,000 years. Without salt, the entire domain would be frozen. Bottom heat flux 40 mW/m^2.

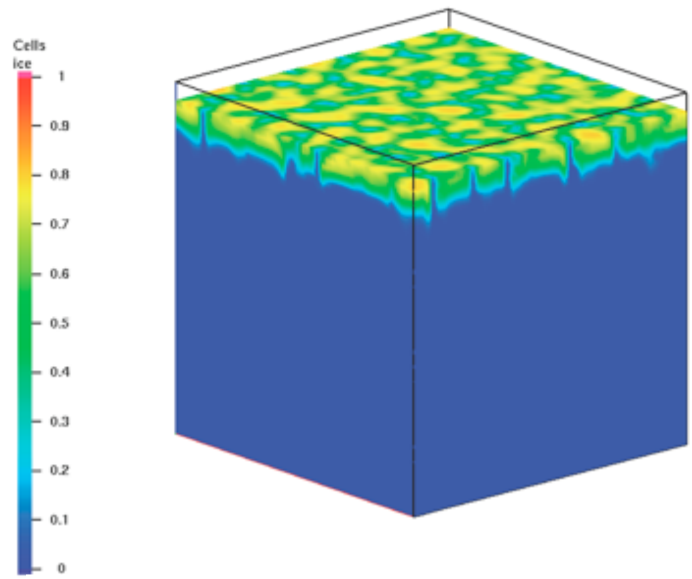

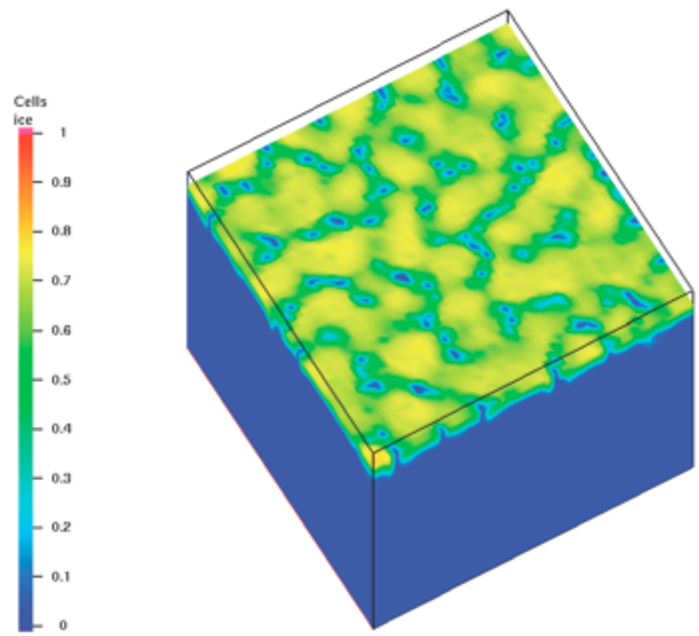

Active Layer & Permafrost System Feedbacks and Variables

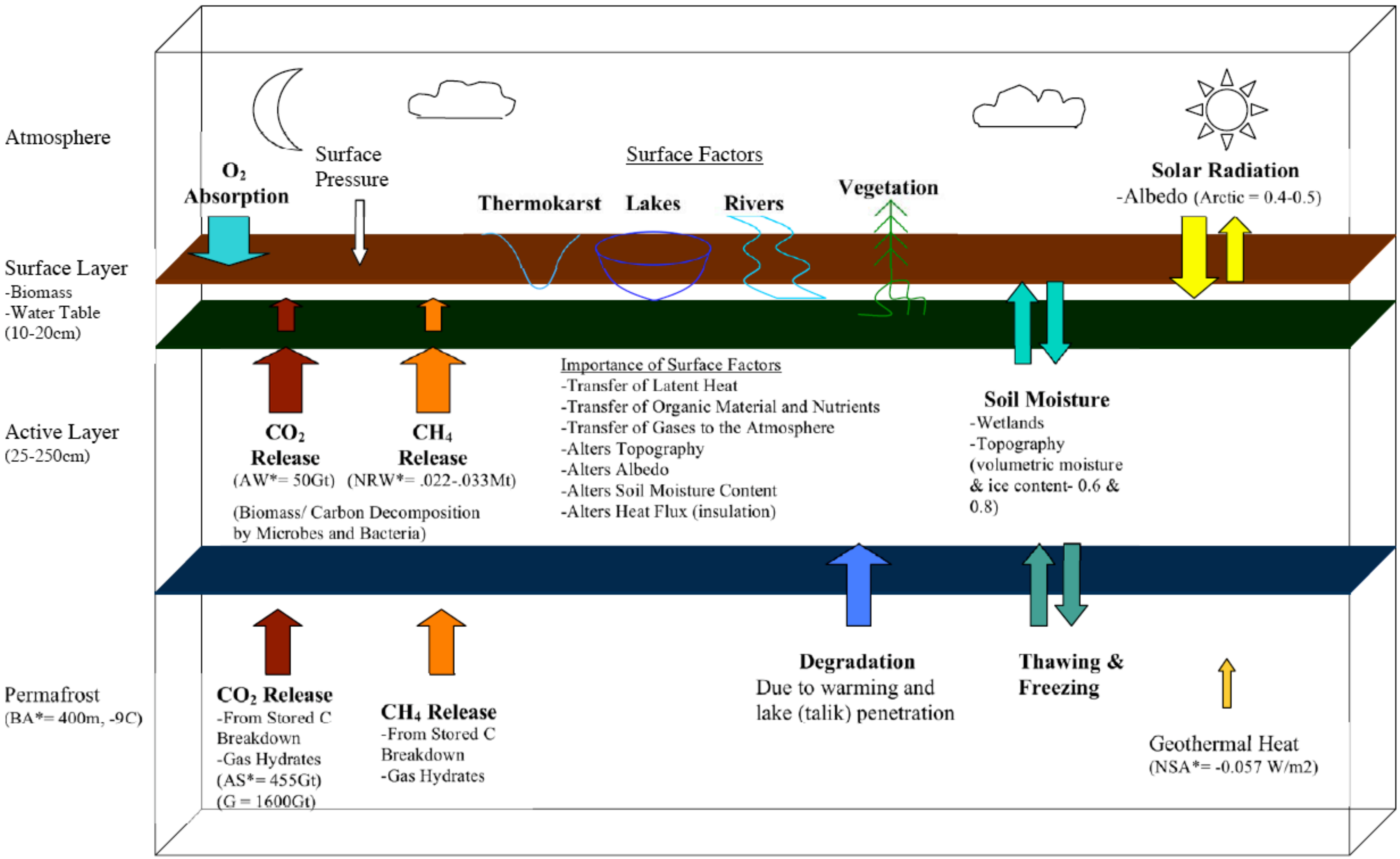

*NRW= Northern Russian Wetlands
*AW= Arctic Wetlands
*AS= Arctic Soils
*BA= Barrow, Alaska
*NSA= North Slope, Alaska
*G = Globally

Image by Irena Ossola

Los Alamos

Deep soil warmed for at least 12 years

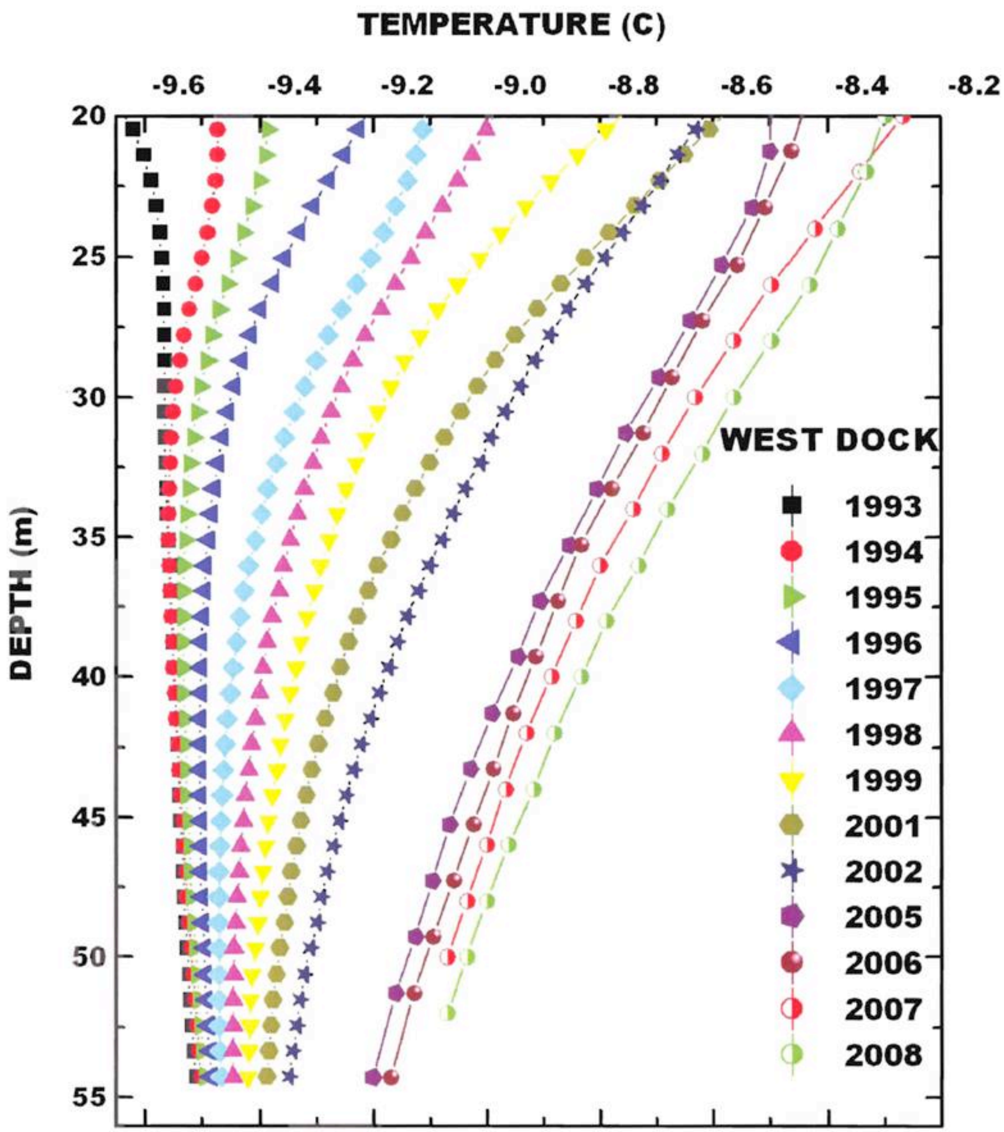

At Prudhoe Bay, from 1993 through 2008 there was a clear increase in temperature at depths from 20 to 55 meters (and below).

While soil at those depths is still solidly frozen, the warming trend is rapid: **+1.3°C in "only" 12 years at 20 m depth!**

NGEE arctic heating experiment sketch

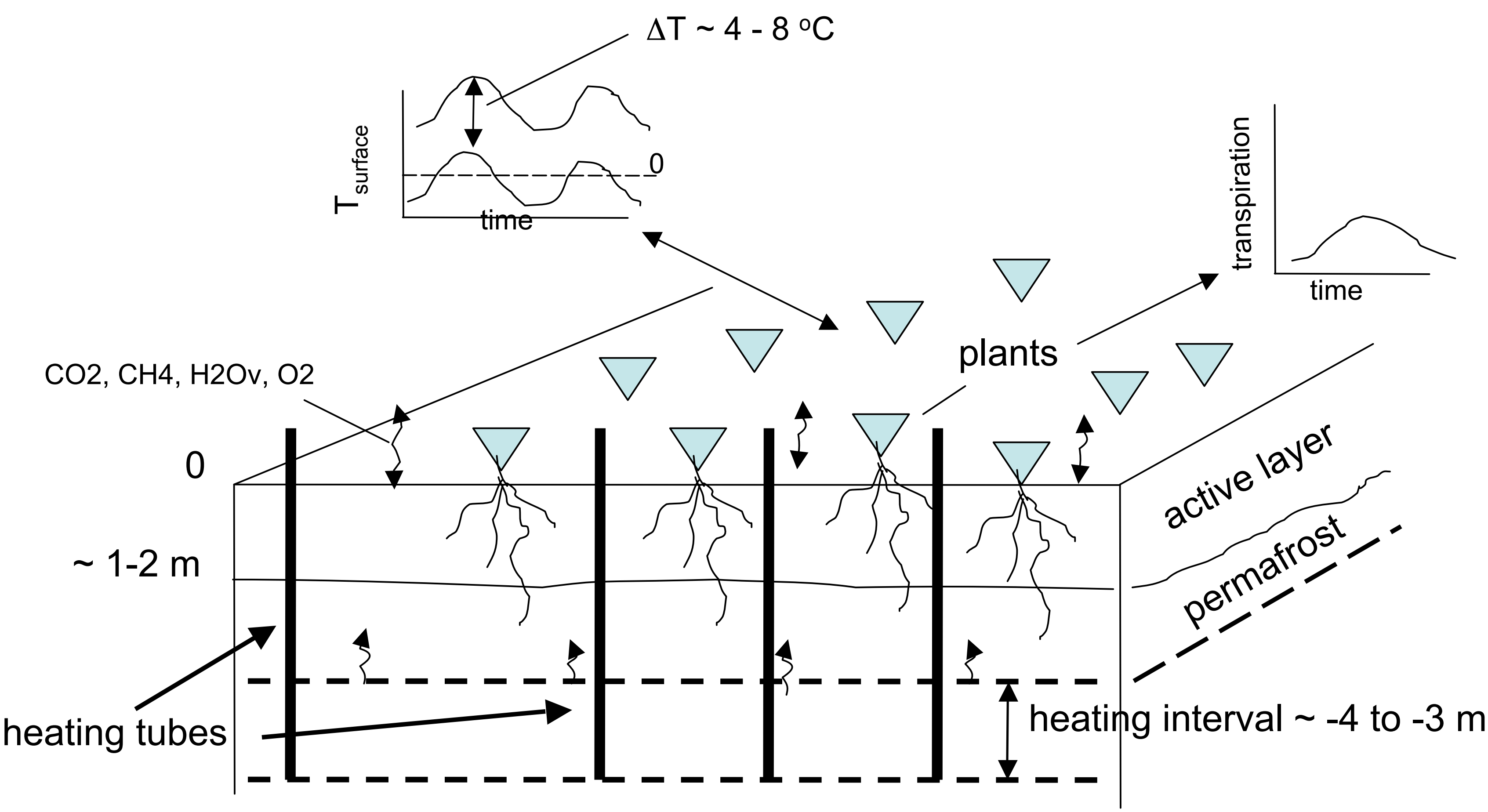

ARCHY model captures several important processes, including heat transport, ice/water phase transition, saturated/unsaturated conditions, simple plant transpiration module, diffusion/advection of gases and water, microbial production of co2, ch4, using 1-D, 2-D or 3-D geometries, plus optimization capability.

Los Alamos

Heat transport, melting/thawing, fluid flow

LANL MAGHNUM/ARCHY codes

NGEE model domain

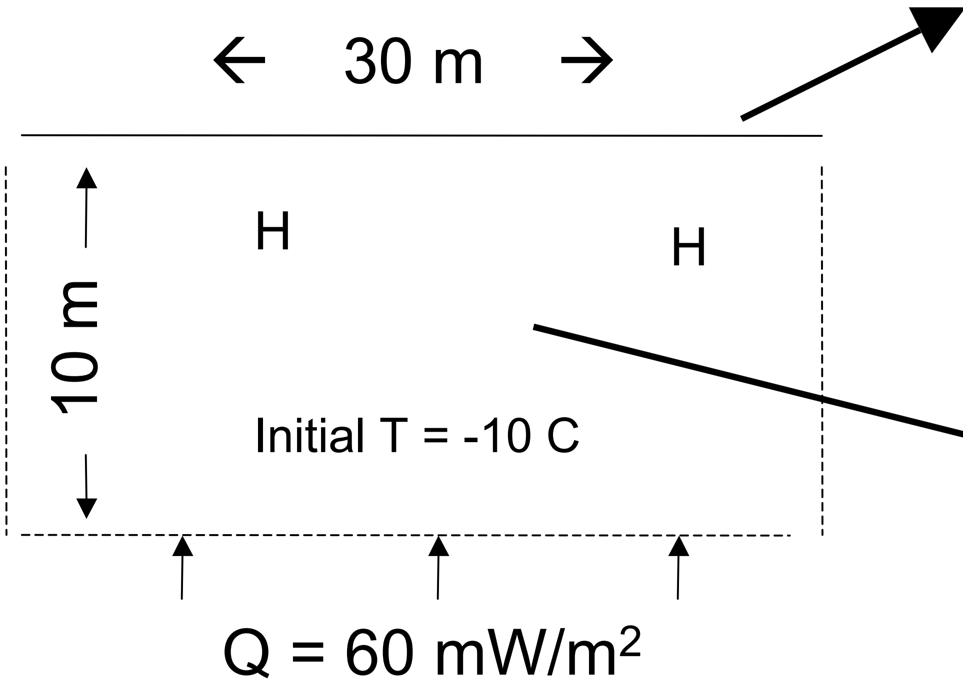

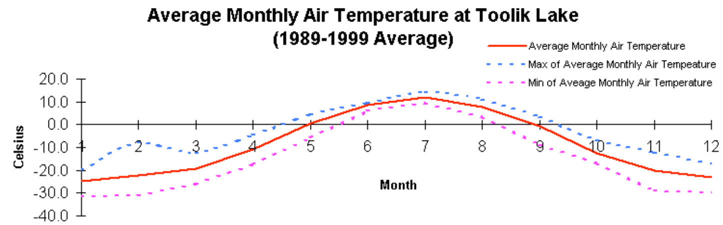

Avg. Monthly Total Rain (mm) 89-99			
Month	Average	Max	Min
June	46.1	61.0	29.5
July	70.0	142.0	12.2
August	64.2	117.9	44.7
Yearly average precipitation - 318 mm			

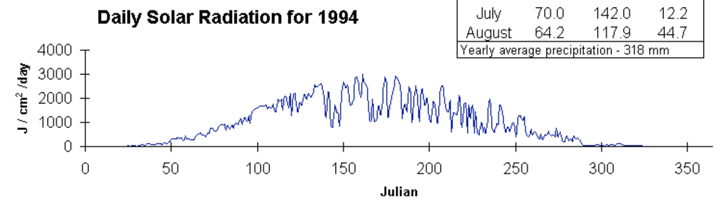

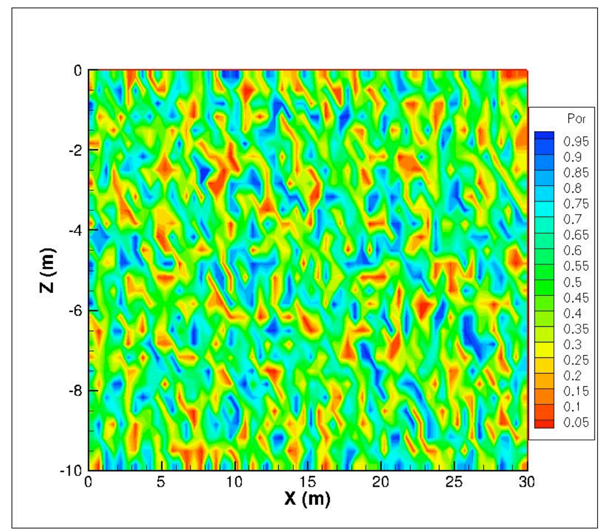

H = heater location; part of study is to see how different heater configurations affect permafrost distribution

Porosity and permeability assumed randomly distributed; pores are water or ice-filled

Los Alamos

Soil Temperatures vs. Time, Data and Model Results

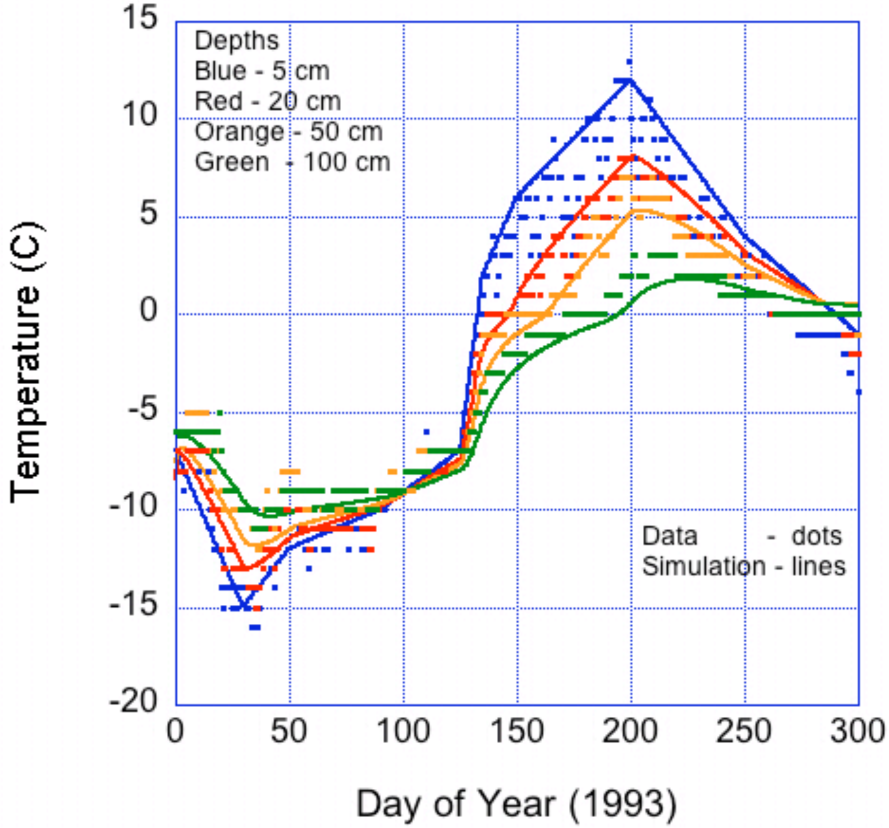

Measured temperatures (symbols) at several depths vs time at a Toolik Lake (Alaska) permafrost experimental site, compared to temperatures computed using the ARCHY model (lines). Surface temperature and precipitation records are applied at upper boundary. Model domain is 5 m deep. Model temperatures at depth track measured values reasonably well. The deepest probe shows somewhat higher temperatures (up to 1 ^{o}C) than the model, indicating the amount of pore ice or thermal conductivity of the soil in the model needs further adjustment. Calibration at Toolik Lake provides us with an opportunity to test and improve the ARCHY model for an arctic NGEE experiment.

Los Alamos

Comparison of ARCHY Simulation (colored) with Jame and Norum

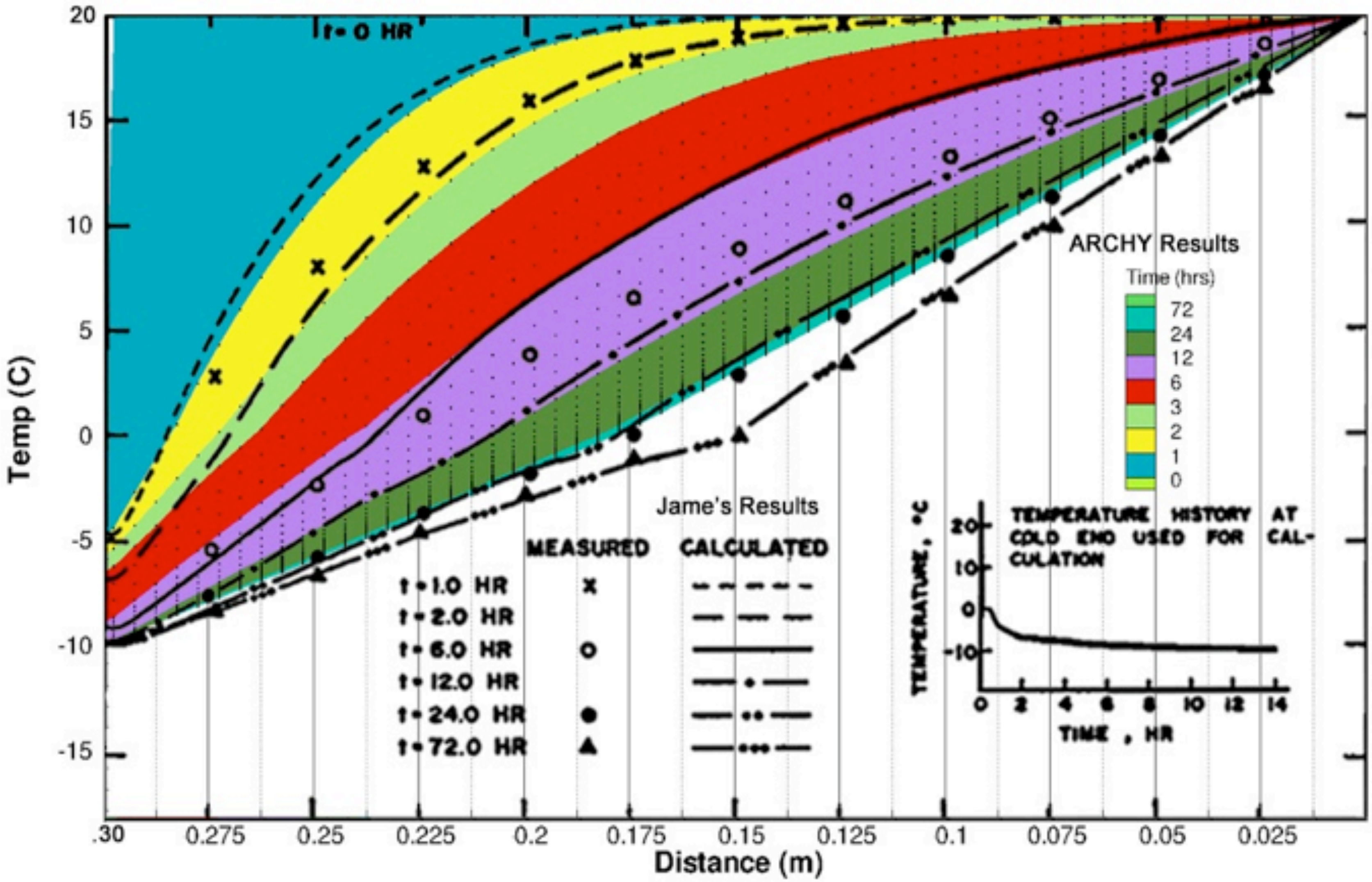

Color bands represent calculated temperatures from ARCHY during the given time intervals. The original experiment consists of a 30 cm column filled with silica with an initial uniform temperature of 20 °C. One end of the column was cooled to 0 °C seperately and then replaced on one end of the column at time = 0. An ARCHY simulation was setup for the experiment and is overlayed here to compare ARCHY with the values measured in the experiment and those calculated by Jame.

Data from Jame & Norum, 1980, Water Resources Res. 16: 811-819.

Simulated Response of Subsurface to Climate Warming Over 50 Year Period

Temperature

Ice Content

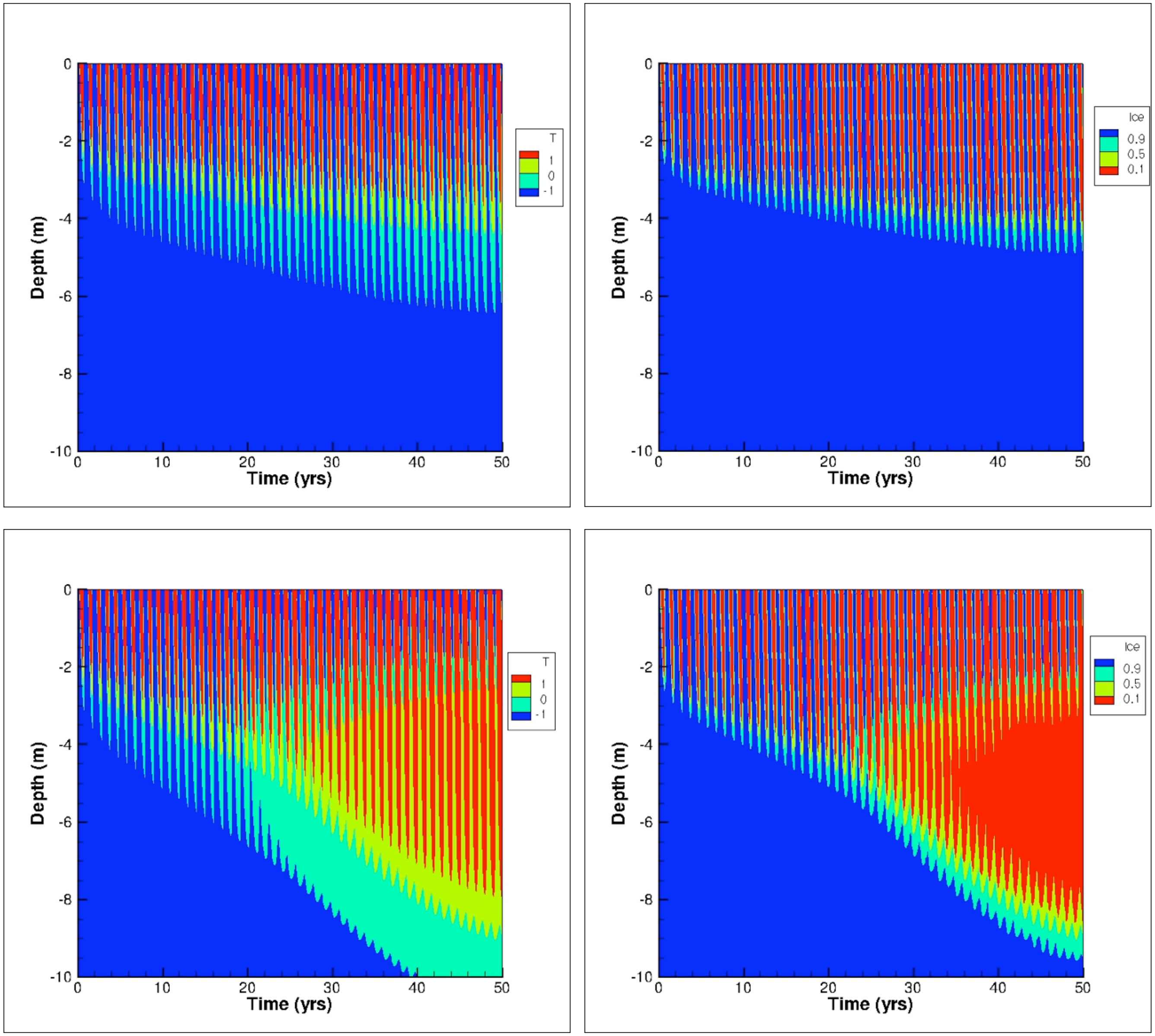

+4 C

Temperature (left) and Ice content (right; blue is frozen, red is thawed) for climate heating from present to +4 C over 50 years (top row) and to +8 C (bottom row). For strong climate warming, a talik region forms at about 4 m depth.

+8 C

Los Alamos
NATIONAL LABORATORY

Minimum and Maximum Temperatures Over Last Year of 50 Year Cycle

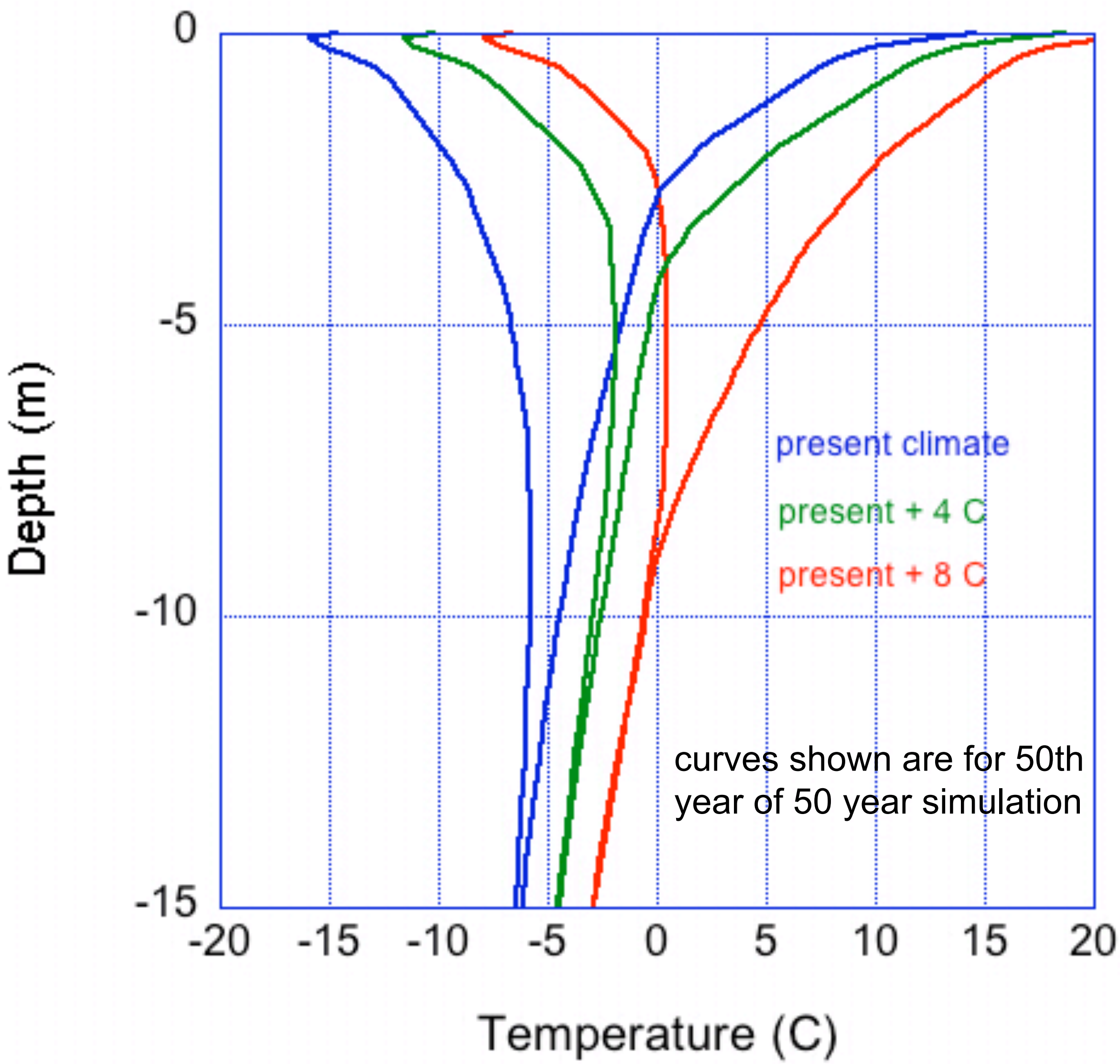

Los Alamos NATIONAL LABORATORY

Thermal Conductivity Varies with the Seasons

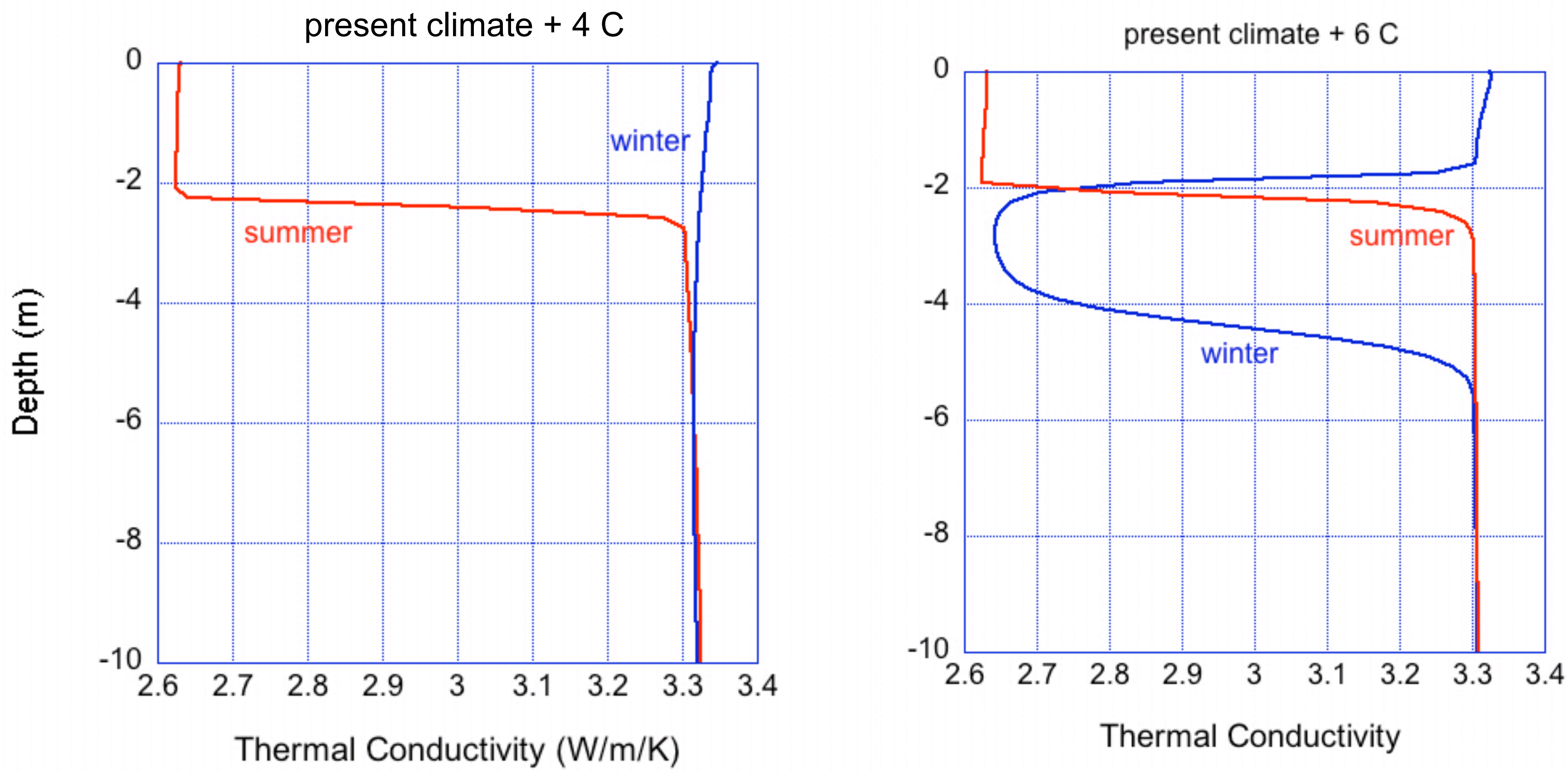

Thermal conductivity is volume averaged over ice content, water content and rock/soil content at each computational node; thermal conductivities of ice and water are significantly different.

Los Alamos
NATIONAL LABORATORY

Biological Activity

Microbes that reside in the soil of the active layer and permafrost can remain active even under cold temperatures of -2 ° to -10° C. It is important to consider soil temperature when calculating and modeling microbial activity as it controls the rate at which respiration can take place. The products of bacterial respiration are what create concern as the large amounts of stored organic carbon are subject to release into the atmosphere as carbon dioxide and methane emissions. Many variables must be considered when calculating the response of microbial activity. Emission levels are particularly subject to soil composition, temperature, moisture and nutrients (such as nitrates and phosphates). The physical properties of the active layer environment are also important to consider as different types of bacteria will interact through symbiotic relationships. Based on these physical properties, the abundance and distribution of aerobic, anaerobic and methanotrophic bacteria within the soil layers determine the concentration of gases produced.

-Methanogens: Bacteria that produce methane under anaerobic conditions from the breakdown of organic carbon in order to produce energy.

Reaction: $CH_3COOH \Rightarrow (1\text{-}x)\ CH4 + (1\text{-}x)\ CO_2 + 2x\ M_{an}$ where $\frac{dM_{an}}{dt} = d_4R_2 - \lambda_{an}M_{an}$

-Aerobes: Bacteria that utilize oxygen to convert organic carbon

Reaction: $CH_3COOH + (2\text{-}x)\ O_2 \Rightarrow$ $(2\text{-}x)\ CO_2 + (2\text{-}x)\ H_2O + x\ M_{ae}$ where $\frac{dM_{ae}}{dt} = d_2R_1 - \lambda_{ae}M_{ae}$

-Methanotrophs: Bacteria that consume methane as their predominant source of carbon and energy.

Reaction: $CH_4 + (2\text{-}x)\ O_2 \Rightarrow (1\text{-}x)\ CO_2 + (2\text{-}x)\ H_2O + x\ M_t$ where $\frac{dM_t}{dt} = d_5R_3 - \lambda_tM_t$

Consumption Rate Formulas

Carbon: Anaerobic: $$R_2 = k_2 M_{an} \left(\frac{I}{I + O_2}\right)\left(\frac{C}{K + C}\right)$$

Aerobic: $$R_1 = k_1 M_{ae} \left(\frac{O_2}{K_{o2} + O_2}\right)\left(\frac{C}{K_c + C}\right)$$

Methanotrophic: $$R_3 = k_3 M_t \left(\frac{CH_4}{K_{CH4} + CH_4}\right)\left(\frac{O_2}{K_{O2} + O_2}\right)$$

CO2: $$\frac{dCO_2}{dt} = aR_1 + bR_2 + c(b_3 R_3)$$

CH4: $$\frac{dCH_4}{dt} = b_2 R_2 - b_3 R_3$$

O2: $$\frac{dO_2}{dt} = -a_2 R_1 - d_3 R_3$$

-The various coefficients in the equations are determined from stoichiometry and experimental data.

Advection Diffusion Reaction Equations

Transport: $$\frac{\partial C_i}{\partial t} + \nabla \cdot (\vec{v} C_i) = \nabla \cdot (D \nabla C_i) - R_i(C_j) + (S)$$

Energy: $$\frac{\partial E}{\partial t} + \nabla \cdot (\vec{v} E) = \nabla \cdot (K_T \nabla T) + \Delta H + W$$

$$\Delta H = l_1 \frac{dC_{ae}}{dt} + l_2 \frac{dC_{an}}{dt} + l_3 \frac{dCH_4}{dt}$$

Microbial Model has been Compared Successfully to Experimental Data For Non-Arctic Environment

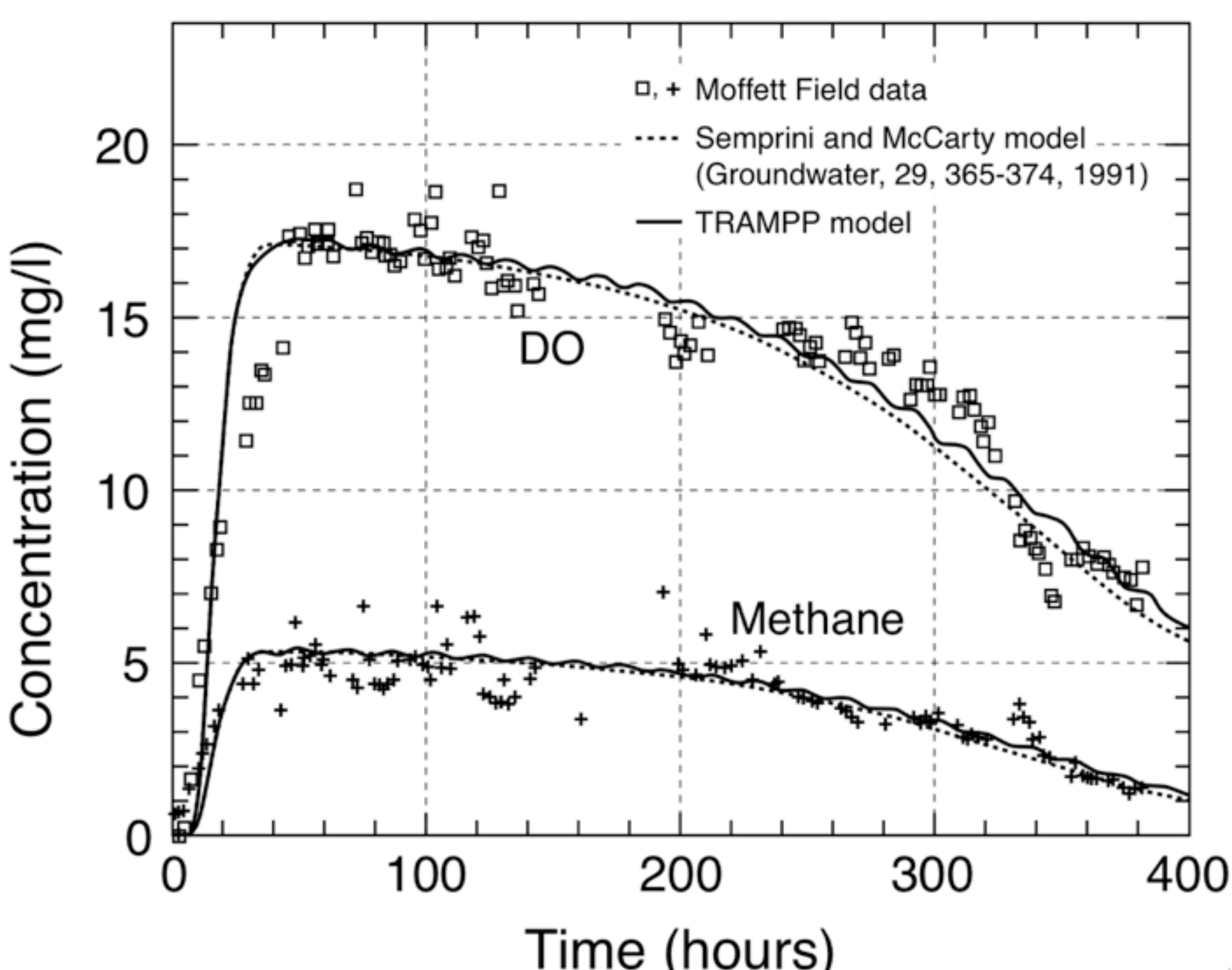

Measured vs Computed Fluxes of CO_2 and CH_4 at an Arctic Site

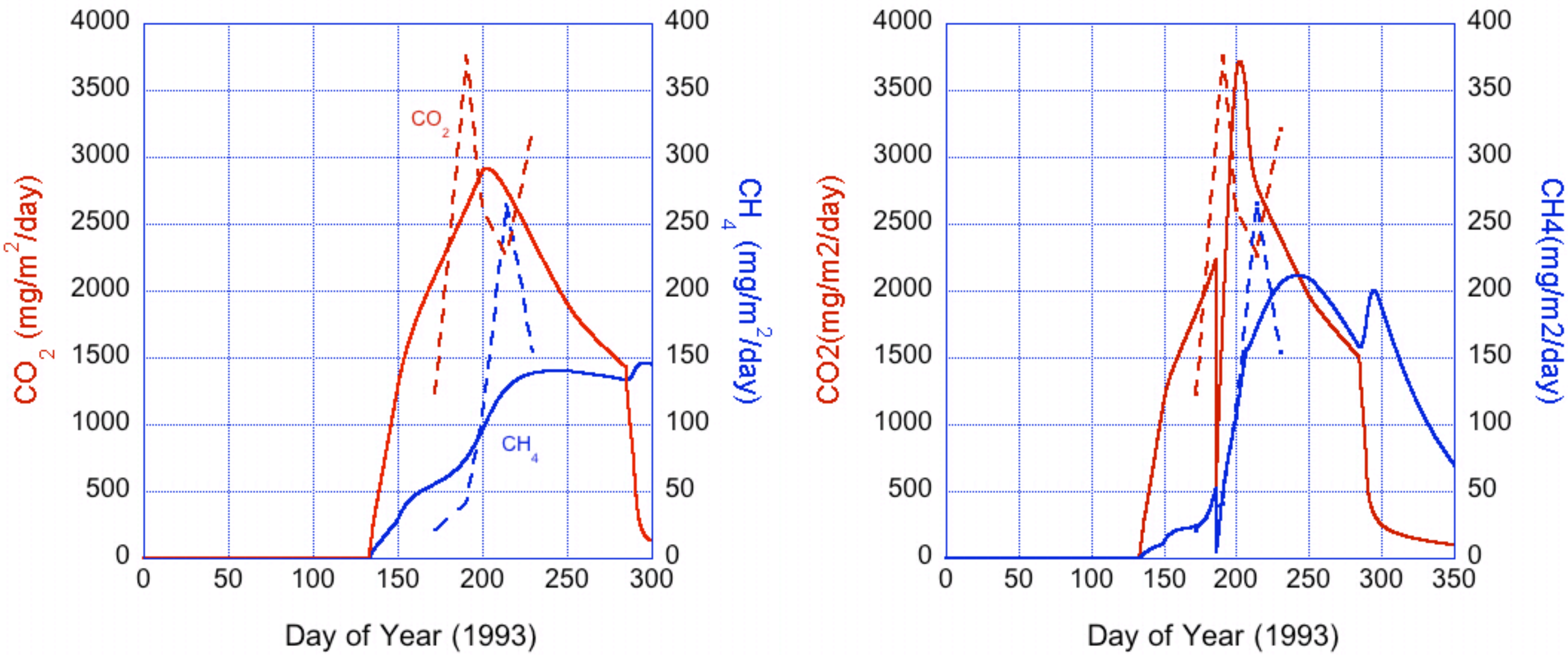

Measured (dashed lines) and simulated (lines) surface fluxes of CO_2 and CH_4 at a Toolik Lake experimental site. Measured surface temperature used as a boundary condition, plus the precipitation record. Left figure does not include a large rainfall event at day 186, right figure does. Temperature and flux data are being used to calibrate the ARCHY model. CO_2 and CH_4 are assumed to be generated by microbial activity. Improvement of the model against data is on-going, as more information about the site is received, and a better understanding of processes develops. Large rain events can significantly alter CO_2 and CH_4 fluxes.

Los Alamos

Active Layer Gas Concentrations and Microbial Populations: Evolution Over 1 Year Temperature Cycle - Present Climate

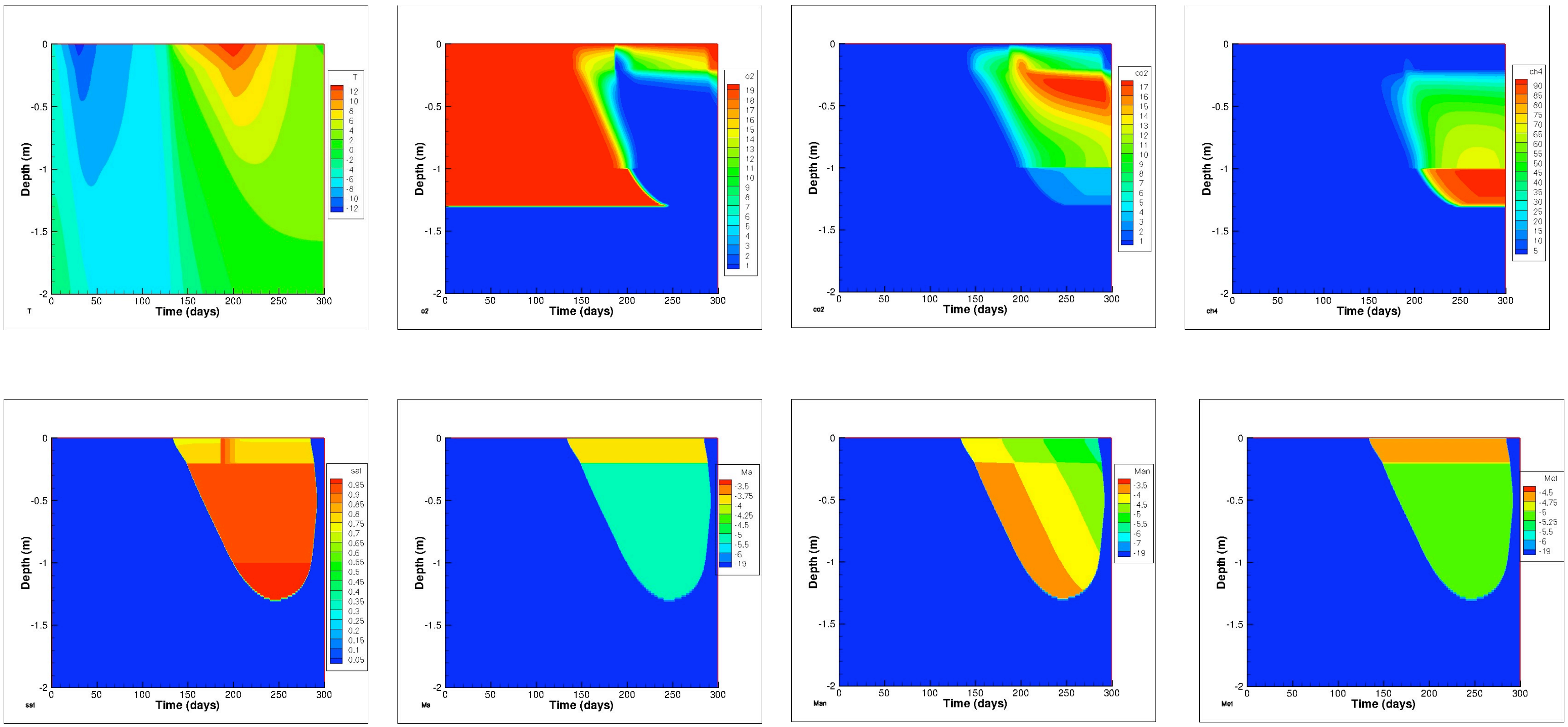

From Irena Ossola (LANL UGS) -
report on Toolik Lake simulations

Los Alamos
NATIONAL LABORATORY

Various Approaches to Multi-scaling

· **Homogenization** – Jikov, Kozlov & Oleinik, 1994

· **Renormalization** – King, 1989; Gavrilenko & Gueguen, 1998

· **Two-scaling** – Keller, 1979; Hou & Wu, 1997; Sviercoski, 2007; Sviercoski, Hyman & Travis, 2008

· **Stochastics** – Neuman, 1994; Di Federico & Neuman, 1997; Guadagnini & Neuman, 1999

· **Wavelets** – Daubechies, 1992; Strang & Nguyen, 1996

· **Lattice Boltzman** – Rothman, 1988; Hazlett, 1995; Zhang et al, 2000

·**Fractals** – Mandelbrot, 1982; Barnsley, 1988; Puente, 1996; Scotti & Meneveau (1997, 1999) for turbulence; Cushman, Benson 1998; Travis, 2001